J Am Soc Nephrol 14: 2188–2198, 2003

Newly Developed Techniques to Study and Diagnose Acute Renal Failure

PIERRE C. DAGHER,* STEFAN HERGET-ROSENTHAL,† STEFAN G. RUEHM,‡ SANG-KYUNG JO,§ ROBERT A. STAR,§ RAJIV AGARWAL,*¶ and BRUCE A. MOLITORIS*¶

**Division of Nephrology, Department of Medicine, Indiana University School of Medicine, Indianapolis, Indiana; Departments of †Nephrology and ‡Diagnostic Radiology, University Hospital Essen, Germany; §Renal Diagnostic and Therapeutic Unit, NIDDK/NIH, Bethesda, Maryland; ¶Roudebush VA Medical Center, Indianapolis, Indiana.*

Abstract. Progress in treating human acute renal failure (ARF) is dependent on developing techniques that allow for the rapid diagnosis, quantification of injury, further understanding of the pathophysiology, and the effects of therapy. Therefore, four techniques that will facilitate this progress are described and illustrated by four different investigative teams. Techniques to measure rapid changes in GFR are available for rapid diagnosis and quantification of ARF in humans. State-of-the-art magnetic resonance imaging (MRI) presently allows for enhanced resolution of regional renal blood flow and functional evaluations in patients. Furthermore, new probes and techniques for MRI that allow for identification and quantitation of inflammation, applicable to human ARF, are being developed and tested in animal models. Finally, two-photon microscopy will allow for four-dimensional cellular and subcellular studies in animal models of ARF providing rapid insights into pathophysiology and the therapeutic effects of a variety of promising agents. Further development and utilization of these techniques, especially in concert with genetic, proteomic, and molecular approaches, will allow for needed insights into the pathophysiology and therapy in human ARF.

Advances in human ARF therapy have been limited to prevention and dialytic support. Interpatient and disease process heterogeneity, as well as a limited number of patients, are barriers to successful interventional therapeutic studies over which there is limited control. However, other relative barriers such as risk factor assessment, early diagnosis and initiation of therapy, and quantitation of ARF severity are now within the reach of clinicians. Quantitation of ARF severity, and the ability to effectively evaluate the response to early therapeutic approaches, are of paramount importance if success is to be achieved. Development of rapid diagnostic tests to allow for randomization of patients on the basis of GFR and ARF severity index is necessary for accurate randomization of patients for therapeutic studies. This, in turn, will minimize interpatient variability and allow for smaller, less expensive, and more reliable studies. To this end, the following four approaches are presented in a very concise format. We have specifically progressed from more clinically applicable techniques to studies aimed at understanding pathophysiologic and therapeutic concepts. Also, many complimentary and powerful investigative techniques have not been discussed. These include the use of "knock out" and "knock in" animal models, genomic and proteomic approaches, and molecular techniques such as silencing RNA and antisense approaches. In combination, these approaches will allow for extremely rapid progress in human ARF diagnosis and therapy.

Estimating GFR Rapidly and Accurately in ARF

Older individuals with a compromised renal reserve and substantial comorbidities are the norm in the hospitalized population. When exposed to nephrotoxins (*e.g.*, radiocontrast, NSAIDs, aminoglycosides) or hemodynamic challenges (*e.g.*, surgery and anesthesia, sepsis, volume depletion), this at-risk population often develops an abrupt decline in GFR. The extent of decline in GFR is known to correlate with the appearance of oliguria (1), and patients with the most impaired renal hemodynamics have the least long-term potential for recovery of renal function (2). Therefore, an accurate estimation of GFR in ARF may be of prognostic importance. This knowledge would also help in stratifying patients into mild, moderate, and severe ARF, which has significance for clinical studies.

The extension phase of ischemic ARF involves alterations in renal perfusion, continued hypoxia, inflammatory processes,

Correspondence to: Dr. Bruce A. Molitoris, Director, Nephrology Division, Indiana University School of Medicine, 1120 South Drive, Fesler Hall 115, Indianapolis, IN 46202. Phone: 317-274-5287; Fax: 317-274-8575; E-mail: bmolitor@iupui.edu

1046-6673/1408-2188
Journal of the American Society of Nephrology

DOI: 10.1097/01.ASN.0000079790.91292.4A

and ongoing epithelial and endothelial injury, primarily in the cortical-medullary region. The extension phase is the time to intervene with interventional therapies (3). Therapeutic maneuvers targeted at improving renal blood flow and regional perfusion are perhaps best detected by measurement of GFR in the clinical setting. Quantifying GFR with sensitive and specific techniques will allow testing of the hypothesis that early therapy modifies the extent and prognosis of renal dysfunction. At the bedside, knowledge of GFR would also be desirable for drug dosing, timing of dialysis, and predicting prognosis.

Although hemodynamic alterations are important in the pathogenesis of ARF, it should be noted that urinary PAH clearance, traditionally used as a test of renal plasma flow, may grossly underestimate renal plasma flow in those with ARF (4). Total renal plasma flow, measured by alternate techniques, is close to normal during the extension, maintenance, and recovery stages of ischemic renal injury. Thus, GFR measurements are of greater value in the setting of ARF.

Pitfalls in the Measurement of GFR in ARF

Measurement and estimation of GFR in ARF presents numerous challenges. Serum creatinine concentration alone will provide inaccurate information of estimated GFR when the GFR is rapidly changing or before it reaching an equilibrium value. Thus equations to estimate creatinine clearance from serum creatinine cannot be used. In addition, clearance also inaccurately estimates true GFR because of tubular secretion of creatinine. Oral cimetidine, a blocker of tubular creatinine secretion, improves the accuracy of measuring creatinine clearance but requires a pretreatment period. In addition, the GFR measurements after cimetidine administration have not been validated in patients with ARF. Urinary clearance of GFR markers may provide better information. Thus, if a bolus of a marker such as inulin was administered intravenously and its urinary clearance measured, an estimate of GFR can be obtained.

The choice of the GFR marker such as inulin, 125-I iothalamate, and others has been validated in patients with stable renal function. These measurements presume the marker is filtered, not metabolized, neither reabsorbed nor secreted by the tubule, and can be reliably measured in the blood and urine. However, with tubular obstruction and backleak, these assumptions may not hold true. For example, increased transcapillary hydraulic pressure gradient and tubular dilatation was the predominant cause of persistent renal failure in patients with ischemic transplanted kidneys (5). Leakage of substances filtered at the glomerulus, but which leak back across the tubular epithelium, may underestimate GFR in ARF. Olbricht *et al.* (6) measured the permeability to those substances most commonly used for filtration rate determination, such as polyfructosan and inulin, by measuring their recoveries after perfusion through various nephron segments in ischemic and nephrotoxic models of ARF in animals. Distal recovery of polyfructosan and inulin were reduced by a maximum of 11%, and urinary recovery of inulin was reduced by only 15% in kidneys showing severely restricted renal function. Thus the reduction in whole kidney inulin or polyfructosan clearance reflects primarily a reduction in GFR, although there is also a small component of backleak.

Techniques of Measurement of GFR in Patients with ARF

GFR is commonly measured using plasma or renal clearance of marker solutes administered as a bolus or continuous infusion. The reference standard is renal inulin clearance, but other solutes commonly used include radioactive (^{125}I-iothalamate [Glofil], ^{51}Cr-EDTA) or non-radioactive markers (iothalamate, iohexol, polyfructosan). Paramagnetic agents (gadolinium DTPA) are rarely used. GFR can be measured by various methods, including the continuous infusion method (IM), the standard clearance method (CM), or the plasma clearance method.

Continuous Infusion Method without Urine Collection

When estimating GFR by the infusion method, a known concentration of GFR marker (IC) is infused at a constant rate (IR), usually following a bolus-loading dose. Since the GFR is often unstable in patients with ARF, a steady state may not be achieved, a major assumption underlying this method. Therefore, this method is not suitable for use in patients with ARF.

Standard Clearance Method with Urine Collection

In calculating GFR by the standard clearance method, bolus and infusion of a GFR marker is carried out in a manner identical to above. In addition, urine is collected at three to six timed intervals of 20 to 30 min each in a water-loaded state. The urine flow rate (V) and urinary iothalamate concentration (U) are recorded. Peripheral venous blood is drawn immediately before and after the urine collection period for measurement of plasma maker concentration (P). P represents the logarithmic average of the marker concentration before and after the collection period. The renal clearance is calculated by the formula:

$$\frac{U \times V}{P} = GFR \qquad (1)$$

This method lends itself well to estimation of GFR in ARF when hemodynamic changes can be rapid. By collecting urine and plasma at timed intervals, rapid changes in GFR can be detected. Using a previously published HPLC technique for measurement of iothalamate(7), the technique was used successfully in following renal hemodynamic changes in patients undergoing unilateral extracorporeal shockwave lithotripsy. A continuous subcutaneous infusion of iothalamate using an insulin pump is started as an outpatient to obtain steady state. Serial measurements of GFR were made before and after lithotripsy. Results from one such patient show a profound fall in GFR that occurs rapidly even when the shock is delivered to only one kidney (Figure1).

Plasma Clearance Method

To calculate plasma clearance, a bolus dose of a marker is administered followed by multiple plasma samples to calculate

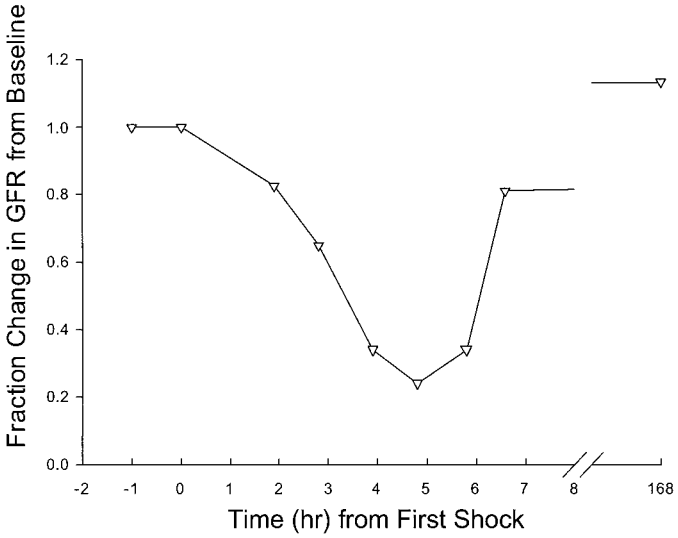

Figure 1. A 35-yr-old white woman with renal stones but no renal failure or hypertension underwent extracorporeal shockwave lithotripsy. Change in GFR from baseline is shown. Time 0 represents the application of first shock to the kidney. At about 7 h, GFR was 80% of baseline and recovered to normal within a week. The measurements were made by measuring renal clearance of iothalamate with urine collections. A Foley catheter was placed for the purpose of collecting timed specimens of urine.

the disappearance rate of the marker (8). GFR measurements using a nonradioactive plasma iothalamate clearance after a single bolus of 3 ml of Conray 60 (1.8 g of iothalamate meglumine) have recently been reported (9). This method uses a rapid and improved assay for iothalamate in plasma and urine.

Erley *et al.* (10) have measured GFR by nonradioactive radiocontrast in critically ill patients using a single injection technique and found good correlation between inulin clearance and limited sampling single shot plasma clearance technique. These authors used radiographic fluorescence, which is less sensitive than the HPLC technique and requires administration of large volume of radiocontrast (11). Accordingly, HPLC techniques, that require lower contrast dose, may be more appropriate to use in patients with ARF.

Simultaneous Renal Imaging and GFR Measurement

Radioactive Markers. 51Cr-EDTA clearance is the most commonly employed GFR marker in Europe (11). Using a slightly different GFR marker, 99m Technetium-diethylene triamine pentaacetic acid (99mTc-DTPA), Rabito *et al.* (12,13) used a radiation detector attached to a miniature data logger to monitor the clearance from the extracellular space. Plasma clearance showed an excellent correlation with simultaneous GFR measurements performed with a standard ^{125}I-iothalamate clearance technique in 50 patients with better reproducibility of the plasma clearance compared with the standard clearance technique. Importantly, renal function was monitored in patients at risk for ARF during angiography or in the intensive care unit under noninvasive and near real-time conditions. The results indicate the technique detects rapid changes in renal function with a resolution time of 5 min in patients with normal renal function and 15 min in patients with severely impaired renal function. Confirmation of the validity of the method may allow noninvasive, precise, and real-time measurement of GFR.

In conclusion, a variety of techniques are available that allow measurement of GFR in patients with ARF. These include radioactive and nonradioactive clearance techniques as well as methods that combine imaging of the kidney with the estimation of GFR. Application of these methods to patients with ARF will allow evaluation of interventions to reverse or stabilize the GFR in ARF and hopefully prevent the morbidity and mortality associated with it.

Magnetic Resonance Imaging in Human Acute Renal Failure

Major goals of renal imaging in acute renal failure (ARF) include detection of urinary tract obstruction and the diagnosis of renal structural abnormalities related to chronic renal disorders underlying ARF. A further goal is to evaluate renal arterial perfusion and venous drainage and their alterations in ARF. Renal imaging in ARF has traditionally been the mainstay of ultrasound including duplex technique as ultrasound has been widely available, inexpensive and easy to apply. In comparison, magnetic resonance imaging (MRI) has only been of minor importance for imaging of ARF. Until the mid 1990s, MRI was limited by its restricted availability, its long acquisition times, and its low spatial resolution (14). In addition, contrast agents for MRI were not yet available and renal perfusion could not adequately be evaluated. Furthermore, non contrast-enhanced MRI of the kidneys has limitations with regards to differentiation of various anatomical structures. The loss of corticomedullary differentiation was described as a common diagnostic finding in acute renal failure in non-contrast MRI (15). However, later studies identified the loss of corticomedullary differentiation in non-contrast enhanced MRI as nonspecific as it may be present in various renal conditions such as glomerulonephritis, obstructive hydronephrosis and other etiologies of chronic renal insufficiency, and acute renal allograft rejection (16).

Recent technical developments in MRI have permitted ultrafast imaging with short acquisition times. Furthermore, imaging with contrast agents based on gadolinium-DTPA has been established, and MR technologies have become widely available (14). The market-introduced gadolinium-chelates are non-nephrotoxic, freely filtered by the glomerulus, and not reabsorbed or secreted by the tubules (17). Therefore, they are well suited to assess GFR. However, gadolinium-chelates are characterized by a short blood residence time, which impedes "steady state" MRI acquisitions beyond the arterial first pass MRI (14). The short blood residence time renders visualization of small vessels, performance of high-resolution MRI, three dimensional image acquisition, and imaging of several vascular regions difficult. These limitations were recently overcome by the introduction of faster gradient systems (18). These recent developments allow for the acquisition of complex

three-dimensional data sets within a single breath-hold. The application of newly developed bolus-chase strategies enable even whole body, three-dimensional magnetic resonance angiography, as shown in Figure 2, in under 2 min (18). Besides detection of urinary tract obstruction or renal parenchymatous abnormalities, vascular, especially arterial, morphology is accurately and rapidly assessed from the supra-aortic to the distal peripheral arteries in one diagnostic procedure. This is of interest, as patients with ARF may also suffer from atherosclerosis or abdominal aortic aneurysms or may present with renal arterial or venous obstruction or occlusion. Information about these comorbidities, as diagnosed by whole body MR angiography, can essentially alter the therapy of patients with ARF.

Some MRI studies investigating intrarenal perfusion in ARF with currently available contrast agents have demonstrated that the loss of corticomedullary differentiation is a sign of changing differential perfusion to the renal cortex and medulla in ARF (17,19). However, there are conflicting studies, which could not demonstrate an association between ARF and loss of corticomedullary differentiation (15). As in native kidneys, MRI may be valuable to distinguish urinary tract obstruction, ARF, vascular complications, and acute allograft rejection after renal transplantation (17). Respective studies have suggested that MRI may lack specificity and thus may be inappropriate to differentiate the etiology of acute allograft dysfunction (16,17,19). However, these studies did not use contrast agents or current MRI technology enabling high image resolution. Therefore, the issue whether MRI is a valuable diagnostic tool in acute allograft dysfunction remains unresolved.

Data indicate that intrarenal small vessel endothelial cell damage may contribute to extend ischemic injury during ARF (3,20). Renal vascular endothelial and smooth muscle cell damage, especially in the corticomedullary region, was shown to cause prolonged hypoperfusion associated with more severe outcomes of ARF. However, these data were predominantly gathered from animal experiments. As recently reviewed, difficulties may arise when results from *in vivo* models regarding pathophysiologic processes in ARF are translated to human ARF (21,22). One of the major obstacles to extending these observations to human ARF is the absence of a non-invasive method to assess small-vessel, regional perfusion and oxygenation within the kidney (3). Despite the advances in MRI technology described above, MRI has not substantially contributed to elucidating the intrarenal vascular pathophysiology in ARF. Perfusion of different regions of the kidney, and its alterations during ARF, seem to be attractive objects for MRI studies. Therefore, new techniques are required to study intrarenal perfusion alterations during ARF. These techniques should permit high resolution to distinguish perfusion changes within different regions as the renal cortex and the medulla in conjunction with rapid image acquisition to assess accurately the dynamics of intrarenal perfusion changes during ARF (Figure 3).

Two MRI techniques have recently emerged that may enhance the studies of the intrarenal perfusion and oxygenation in human ARF - blood oxygenation level-dependent (BOLD) contrast MRI and MRI with blood pool contrast agents. BOLD

Figure 2. Whole-body three-dimensional (3D) MR angiogram in a 57-yr-old male patient showing diffuse manifestation of atherosclerotic disease with high-grade stenoses of supra-aortic and bilateral carotid arteries, exulcerated plaque of suprarenal aorta, caliber irregularities and stenosis of infrarenal aorta, high-grade stenoses, and occlusions of bilateral superficial femoral arteries. In addition, high-grade stenoses of bilateral renal arteries are depicted, with consecutive shrinking of the kidney on the left side. The whole-body MR angiography concept is based on the acquisition of five slightly overlapping 3D data sets acquired in immediate succession after the intravenous injection of paramagnetic contrast agent. The total data acquisition time amounts to only 72 s. The technique allows for rapid non-invasive assessment of the arterial vessels from supra-aortic arteries to the distal runoff vessels including the renal arteries.

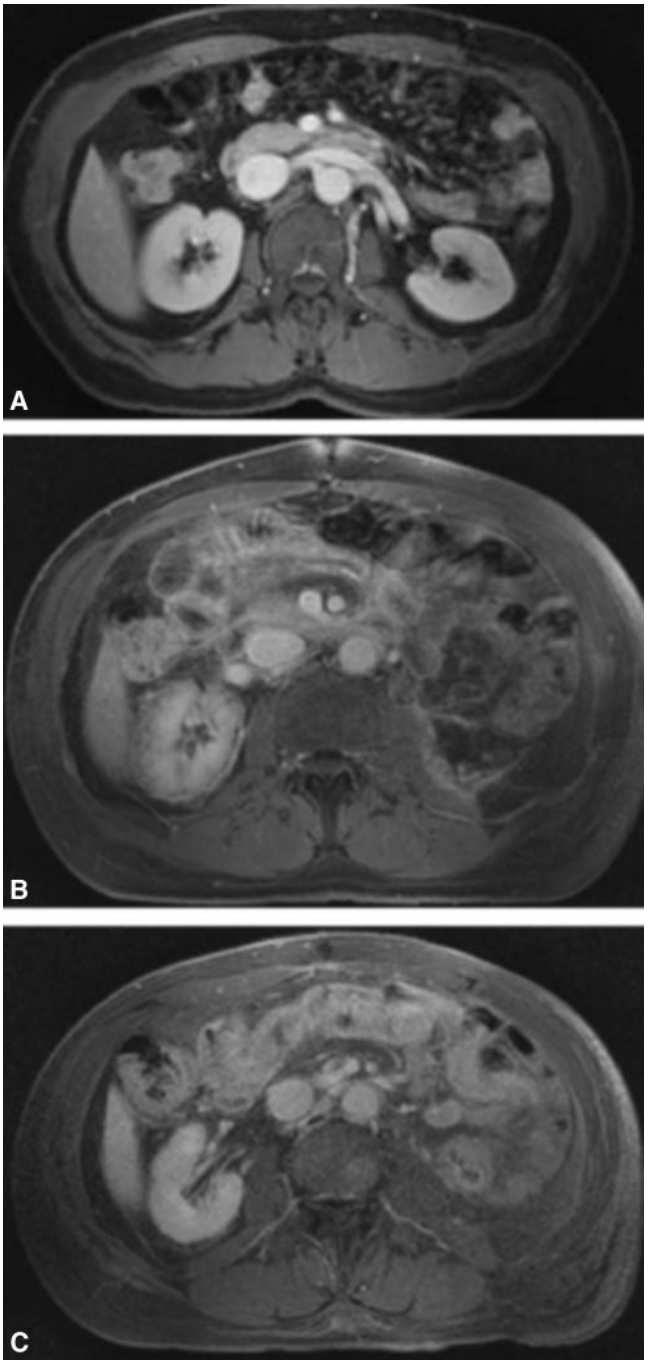

Figure 3. Contrast enhanced MR imaging with gadolinium-chelates of the kidneys in a 60-yr-old male patient who developed acute renal failure after left-sided nephrectomy for living related renal transplantation. (A) Preoperative imaging showed regular perfusion of both kidneys. (B) Two days post nephrectomy, the patient developed ischemic acute renal failure. The remaining right kidney showed medullary hypoperfusion and a cortical rim of decreased perfusion. (C) Three-week follow-up study shows complete recovery with reconstituted homogeneous perfusion of the right kidney.

MRI depends on the principle that hemoglobin (because of its iron content) changes its magnetic qualities depending on whether hemoglobin is in the deoxygenated or the oxygenated form (23). Deoxyhemoglobin shows paramagnetic, oxyhemoglobin diamagnetic effects in the magnetic field. Therefore, deoxyhemoglobin acts as an endogenous contrast agent, and increased deoxyhemoglobin concentration leads to signal attenuation in T2 weighted MR sequences. Because the ratio of deoxyhemoglobin to oxyhemoglobin is related to the pO_2 of blood, which again is thought to be in equilibrium with the surrounding tissue, BOLD MRI can noninvasively estimate tissue pO_2 in humans (23,24). By BOLD MRI techniques, marked hypoxia of the medulla was recently demonstrated during ARF (23). BOLD MRI is limited, as it measures intrarenal oxygenation and not perfusion. Therefore, BOLD MRI cannot distinguish between alternating oxygenation induced by changing perfusion or by oxygen consumption (24). Additionally, BOLD MRI involves complex mathematical data processing that may limit its widespread clinical use.

Blood pool contrast agents are characterized by prolonged blood residence time and largely reduced interstitial diffusion in comparison with market-introduced gadolinium-chelate contrast agents (14). These features permit steady-state MRI acquisition after the arterial first pass MRI with better visualization of smaller vessels (14). Once available, blood pool contrast agents will improve high-resolution MRI with higher spatial and contrast resolution and three-dimensional image acquisition. Initial studies on MRI with blood pool contrast agents in ARF demonstrated this technique detects medullary perfusion defects and can accurately differentiate between cortical and medullary perfusion with high temporal resolution (25,26). Even moderate perfusion changes in different intrarenal regions were clearly visible with blood pool contrast agents (25). Despite the unresolved issue of potential toxicity of blood pool contrast agents, current MRI technology together with blood pool contrast agents appears to offer most advantages to study vascular pathophysiology in human ARF.

As discussed, recent advances in MRI may further improve the early and accurate detection of ARF etiology and of important comorbidity. In addition, emerging MRI techniques may offer new insights into intrarenal, small vessel alterations in human ARF with high temporal and spatial resolution. MRI may also facilitate the evaluation and monitoring of future therapies targeted to ameliorate endothelial injury and dysfunction in ARF.

MRI Methods for Understanding the Pathogenesis of Acute Renal Failure

Although a number of pathogenic mechanisms have been identified in animal models of ARF, the pathogenesis of human ARF is still unknown; perhaps as a result, there are no FDA-approved drugs for the prevention or treatment of clinical ARF (27,28). Determining the pathophysiology of human ARF has been difficult because of the paucity of renal biopsies, especially in early ARF (22,29). Hence, the site of renal injury (proximal *versus* distal) and the role of inflammation in human ARF remain uncertain. Direct detection of early proximal tubule dysfunction, an important site of injury in some ischemic and nephrotoxic models (27), would be extremely helpful. Similarly, non-invasive detection of significant leukocyte

accumulation would implicate inflammation as a potential therapeutic target. Non-invasive imaging techniques such as renal ultrasound, duplex Doppler ultrasound, and CT imaging are used clinically to detect urinary tract obstruction and measure renal perfusion. Unfortunately, these techniques cannot determine the cause of ARF, nor can they detect dysfunction of specific nephron segments.

Two micro-MRI methods have recently been developed that measure tubular function and renal inflammation in mice and rats, respectively. The first method employs a positive contrast agent that accumulates in the proximal straight tubule (26), whereas the latter method detects a negative contrast agent that is engulfed by infiltrating macrophages (30). It is hoped that these new MR techniques might aid the development of effective therapeutics for human ARF.

Proximal Tubule Dysfunction. The first technique uses dendrimer-based contrast agents to directly detect dysfunction of the proximal tubule, the primary site of renal injury in many renal injury models. Dendrimers are highly branched molecules that can be synthesized with precisely defined molecular size and surface characteristics. Drs. Martin Brechbiel and Hisataka Kobayashi of the National Cancer Institute had synthesized and studied several Gd-dendrimer chelates to image tumor blood vessels and target drug delivery to tumors. MRI contrast agents constructed from the smaller generation-4 dendrimer cores are quickly cleared by glomerular filtration and accumulate in the kidney. Simultaneous injection with lysine inhibits renal accumulation and accelerates their renal excretion (31), suggesting they are filtered, absorbed by the proximal tubule, and accumulate in the proximal tubules. Using a newly developed high-resolution whole body 3-D micro-MR imaging method developed by Dr. Kobayashi, 160-micron spatial resolution was obtained using a 1.5T clinical MRI unit (26). After the vascular blush phase, there were alternating light and dark bands in the cortex and outer medulla (Figure 4), and early filling of inner medulla and urine in the renal pelvis within 2 min post-injection. The layered appearance was noticeable even on the first image, but it was more clearly developed by 5 min after injection. By comparing the micro-MR images with histologic sections, the bright bands were localized to the superficial (sub-capsular) cortex, the outer stripe of the outer medulla with projections into the deep cortical region (the medullary rays), and the urinary space that encompassed the inner medulla and the inner portion of the inner stripe. Thus, the middle white band corresponded to the outer stripe of the outer medulla and medullary rays where the proximal straight tubules are located. The spectacular images of the mouse kidney were achieved because of the high contrast of the agent and improvements in MR imaging.

Proximal tubule dysfunction induced with cisplatin, a chemotherapeutic agent that produces dose-dependent apoptosis and necrosis of the proximal straight tubule, was then studied (32). Following cisplatin administration, there were discernible changes in the G4-dendrimer–enhanced micro-MRI image that corresponded to the known nephrotoxic effects of cisplatin. In animals with mild cisplatin ARF, the outer stripe bright band did not appear, and urinary excretion of contrast agent was delayed. Animals with severe cisplatin toxicity did not accumulate the contrast agent in the outer medulla, nor did they excrete it into the urine. The gradation of tubular damage as assessed by MRI correlated with renal function. Thus, the MRI image can be used to detect damage to the proximal straight

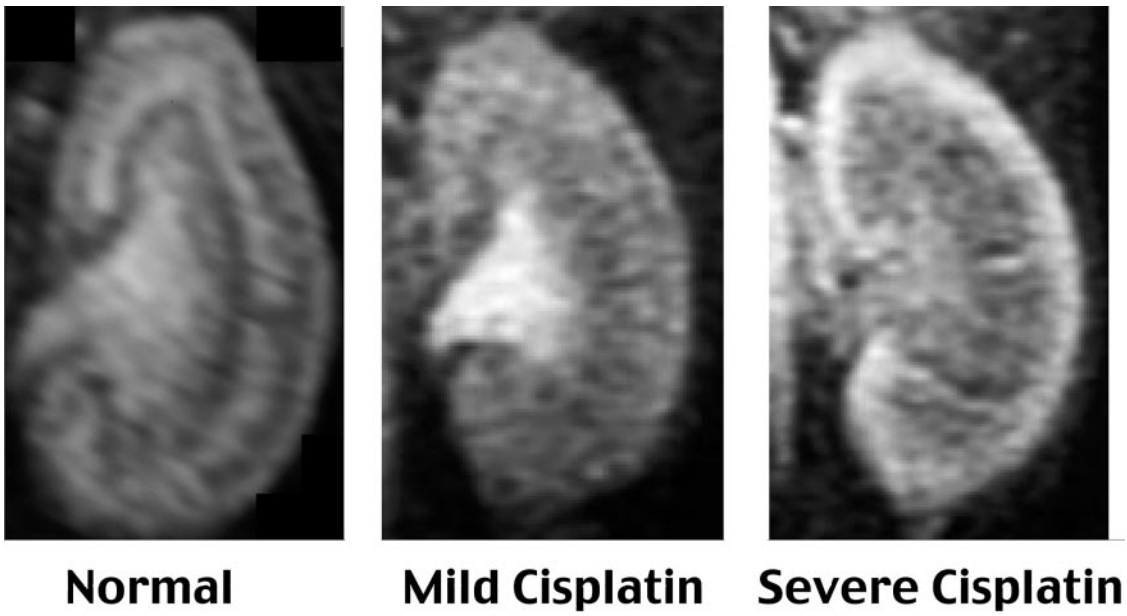

Figure 4. G4 dendrimer–enhanced fat-suppressed T1-weighted micro-MR imaging in mice. Normal mice or mice treated with cisplatin were injected with Gd-labeled G4 dendrimer. Images taken approximately 5 min after injection. Gd-labeled G4 dendrimer accumulates in outer cortex, outer stripe of the outer medulla, and inner medulla/urinary space in normal animals. Cisplatin injury causes decrease in outer stripe accumulation (mild and severe injury) and urinary appearance (sever injury).

tubule (outer stripe white band), and decreases in kidney function (renal transit time). G4-denderimer–enhanced MRI imaging can also detect renal injury in other types of acute and chronic renal injury. For example, the outer stripe accumulation and urinary excretion of G4-dendrimer is lost as early as 2 h after renal ischemia, a second type of renal injury of the proximal straight tubule, and also after renal obstruction (33). Unfortunately, the G4 D dendrimers are retained in the kidney, which might increase the risk of nephrotoxicity. However, a 20-dendrimer library with different sizes and core structures was constructed, and a G2 PAMAM–based dendrimer and two DAB-based dendrimers was excreted almost as rapidly as Gd-DTPA (34), but still have preserved imaging features (33). Thus, dendrimer-enhanced MRI may prove to be a useful tool for non-invasive observation of renal structure and function. In animals, this method might be useful to non-invasive screening of kidney or proximal tubule function after injury, determine the effectiveness of experimental therapies on proximal tubule injury, or search for alterations in proximal tubule and kidney function in transgenic or knockout mice. A Gd-based dendrimer (Gd-BOPTA) is approved in Europe for use in liver imaging.

Detection of Renal Inflammation. In animals, inflammation plays an important role in ischemic and cisplatin-induced ARF, but not following a pure nephrotoxic ARF such as mercury chloride (35). Despite a large body of evidence in experimental animals, the role of inflammation in human ARF is still unknown, again because of the paucity of renal biopsies in ARF. Recent advances in MR imaging using negative imaging agents, such as dextran-coated ultra-small superparamagnetic iron oxide (USPIO) particles, have allowed the detection of inflammation in animal models of cerebral ischemia, arthritis, nephrotoxic nephritis (36), and renal transplant rejection (37,38). The small dextran-coated iron particles are internalized by monocytes and macrophages, and locally degrade the T2*-weighted MR signal. For example, severe transplant rejection produces a nearly black kidney at day 5 because of the large number of infiltrating inflammatory cells (37,38). However, the inflammation after renal ischemia is more subtle, with small foci of inflammatory cells, predominately monocytes and macrophages, in the ascending vasa recta (39). To test if USPIO imaging could detect this smaller amount of inflammation, rats were subjected to renal ischemia and injected with ferumodextran-10 USPIO particles 24 h before MRI, allowing sufficient time for the macrophages to engulf the particles (30). In kidneys subjected to ischemia reperfusion, a black band in the outer medulla was detected at 48 to 120 h after ischemia (Figure 5). This outer stripe band was located at the site of maximal inflammation in the ischemia/reperfusion model, which is also the site of maximal damage to the proximal tubule (see Figure 4). The black band was found after either 40 or 60 min of ischemia (Figure 5), indicating that the method could detect the inflammation present after moderate or severe ischemic injury. In contrast, the band was not detected in normal animals or in animals injected with mercuric chloride, which causes a pure nephrotoxic renal injury with minimal amounts of inflammation (35). The change in signal intensity correlated with serum creatinine and the number of iron particle containing cells detected by histochemical stain (30). The iron particles labeled infiltrating tissue macrophages by light microcopy, and where detected within lysosomes by transmission electron microcopy. USPIO particles did not cause renal injury in normal rats, nor did they potentiate renal injury or prolong the recovery phase in animals subjected to either moderate or severe ischemia (30). Currently, ferumodextran-10 USPIO reagents are being tested for MR lymphography in phase III trials; it may soon be possible to apply this method to patients with ARF.

Clinical Implications. The site of renal injury, existence, and the role of inflammation in human ARF are still unknown. Renal biopsies in patients with ARF could provide some information, but ti would still be limited by sampling error and

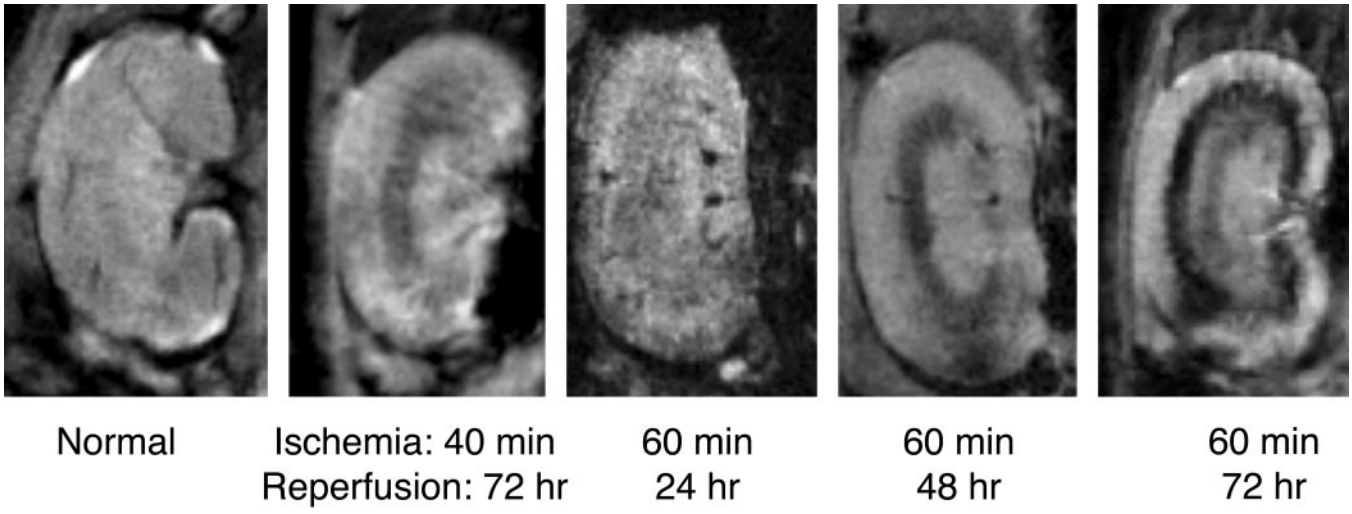

Figure 5. T2*-weighted gradient-echo MR image 24 h after injection of ferumodextran-10 USPIO particles. Rats were normal or subjected to 40 or 60 min of bilateral ischemia. Rats were injected with ferumodextran-10 USPIO particles at 24 h before the time indicated.

difficulty in obtaining outer medullary tissue. Hence, the ability to non-invasively track injury and inflammation would be quite useful in understanding the pathogenic mechanisms involved in human ARF. MRI can examine the entire kidney repeatedly and non-invasively. Dendrimer-based MR contrast agents can non-invasively detect proximal tubule dysfunction, and hence, might be clinically useful to establish the extent of proximal tubule injury in human ARF. While too cumbersome to be used on a routine basis, dendrimer-based MRI could be efficacious for the non-invasive and early diagnosis of acute renal injury in sepsis, or after experimental therapies or procedures. USPIO particles might be useful to determine if inflammation is present in ARF due to ischemic, nephrotoxic, or septic insults. It is hoped that these agents will aid in the development of drugs to prevent or treat ARF by increasing our understanding of the pathogenesis of human ARF.

Imaging Apoptosis Intravitally with Two-Photon Fluorescence Microscopy

Two-photon fluorescence microscopy is an emerging powerful tool that can be applied to image various physiologic and pathophysiologic processes in live animals at the subcellular level (40). The use of near-infrared light allows for deeper tissue penetration and minimizes light scatter encountered within biologic tissues. It also permits the imaging of multiple fluorophores simultaneously due to the significant overlap in long wavelengths utilized to stimulate different fluorescence probes (41). It can take advantage of tissue autofluorescence, injected fluorescence markers, or the fluorescence-tagged proteins in transfected or transgenic animals. Because excitation occurs at only one point in space, where two photons meet to excite the fluorescence probe, the potential for tissue phototoxicity is markedly reduced. Increasingly powerful and fast lasers can then open near real-time views into deeper sections of tissues and organs of live animals. This approach, supported by highly sophisticated acquisition and volume reconstruction software, has been successfully used in some recent publications, and its application is likely to develop at an accelerated rate (42,43). Thus, two-photon microscopy promises to yield a unique picture of the temporal and spatial unfolding of various processes in complex organs of live animals. Therefore, it allows one to approach questions previously not possible. This is especially important for understanding the contributions of and interactions among vascular, epithelial, and inflammatory components to the pathophysiology and treatment of ARF.

An example of the important application of two-photon microscopy is for the study of apoptosis in live animals. Apoptosis is emerging as a central biologic mode of cell death that plays a crucial role in shaping the developing embryo and also in the daily cellular turnover and homeostasis of tissues and organs (44,45). Furthermore, apoptosis seems to be a predominant mode of cell demise in a wide spectrum of pathologic conditions. These include ischemic injury, neurodegenerative diseases, and many immunodeficiency and autoimmune syndromes. Finally, deregulation of the apoptotic program has been strongly implicated in the genesis of many neoplastic conditions and some autoimmune states.

Despite all the advances in the biochemistry and molecular biology of apoptosis, we still lack fundamental knowledge about the exact occurrence and quantitative importance of apoptotic cell death in complex tissues and organs. Our current insights, derived primarily from studies performed on tissue sections after fixation, yield a very incomplete view of apoptosis as it unfolds in the living organism. A series of questions will help illustrate the many problems that cannot be answered easily using fixed tissues sections. Ischemic renal injury will be used as an illustrative example: At what rate(s) and for how long does apoptosis progress in the kidney after ischemia? What are the temporal and spatial relationships between apoptosis and inflammation? What are the temporal and spatial relationships among tubular, endothelial, and inflammatory cell apoptosis? What is the role of apoptotic tubular and endothelial cell death in generating casts, tubular, and vascular leaks? What is the spatial and temporal relationship of apoptosis to areas of nephron regeneration? These and many other questions can be examined only with great difficulty in static sections harvested at fixed time points from the ischemic kidney. What is needed instead is a dynamic four-dimensional view that follows the unfolding of apoptosis in a kidney volume over time. Only then will we be able to assess the quantitative importance of this mode of cell death in this and other highly complex organs and tissues.

The technical difficulties with live imaging are not trivial and range from the point of contact between the tissue and the objective down to the choice of fluorescence markers (42). The delineation of a particular volume in a tissue to be imaged through successive planes over time is also a real challenge that will be overcome at variable rates depending on the organ being imaged. Thus, imaging the beating heart offers a special challenge compared with the more grossly static liver or kidney. The careful choice of fluorescence markers is also crucial to avoid spectral overlap when multiple fluorescence probes are used. Also, the cytotoxicity of these markers and dyes has to be examined very carefully over the time course of the experiment. So far, several common markers have been successfully delivered to tissues via systemic administration with no apparent short-term toxicity. These include propidium iodide and Hoechst to study apoptotic nuclear morphology (Figure 6) and annexin derivatives to evaluate phosphatidyl serine externalization (46,47). Recently described cell permeable fluorescence caspase markers are also very promising in this regard (48). All these can be used in conjunction with probes for specific compartments in the organ like fluorescence large and small molecular weight dextrans to delineate vascular and tubular spaces (following filtration) in the kidney for example (42). Finally, markers of physiologic functions and parameters like cell pH, calcium, or endocytosis can also be imaged simultaneously to assess their roles during the cellular processes. Thus these developing techniques in two-photon live imaging will broaden our understanding of the role of many cellular events in tissue pathology and will thus permit the

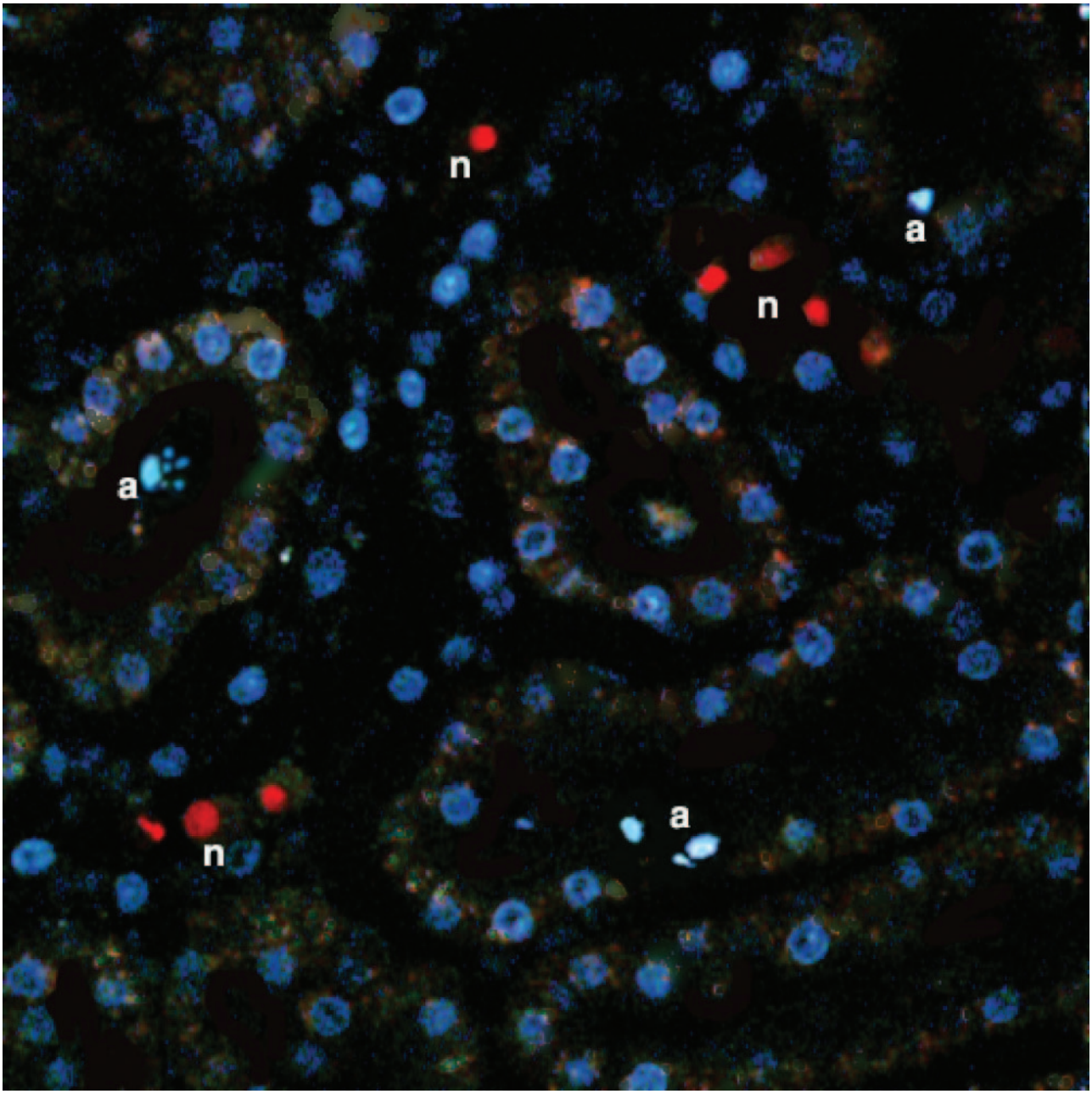

Figure 6. Apoptosis and necrosis viewed with two-photon imaging in a cisplatin model of renal injury. Rat was treated with cisplatin 5 mg/kg intraperitoneally for 3 d before imaging. Propidium iodide (20 μg intravenously) and Hoechst (500 μg intravenously) were administered 30 min before two-photon imaging of the exposed kidney in the live anesthetized animal. A mixture of apoptotic cells (labeled a, with condensed and fragmented nuclei staining intensely blue with Hoechst) and necrotic cells (labeled n, with homogeneous red propidium iodide staining) can be seen.

design of more rational approaches to its modulation. They will also play an essential role in designing and evaluating therapies for specific disease processes.

In summary, techniques are now being developed and utilized that will allow for the rapid diagnosis of human ARF, further understanding of the pathophysiology of human ARF, and insight into the effectiveness of therapeutic agents. The four outlined approaches in this article, in conjunction with maturing work involving genomic and proteomic approaches to risk stratifying patients and ARF marker development, along with new animal models and molecular approaches (RNA, for example) will result in rapid advances in understanding the pathophysiology, diagnosis, and treatment of human ARF.

References

1. Allgren RL, Marbury TC, Rahman SN, Weisberg LS, Fenves AZ, Lafayette RA, Sweet RM, Genter FC, Kurnik BR, Conger

JD, Sayegh MH: Anaritide in acute tubular necrosis. Auriculin Anaritide Acute Renal Failure Study Group. *N Engl J Med* 336: 828–834, 1997
2. Ilic S, Rajic M, Vlajkovic M, Bogicevic M, Stefanovic V: The predictive value of 131I:hippurate clearance in the prognosis of acute renal failure. *Ren Fail* 22: 581–589, 2000
3. Sutton TA, Fisher CJ, Molitoris BA: Microvascular endothelial injury and dysfunction during ischemic acute renal failure. *Kidney Int* 62: 1539–1549, 2002
4. Corrigan G, Ramaswamy D, Kwon O, Sommer FG, Alfrey EJ, Dafoe DC, Olshen RA, Scandling JD, Myers BD: PAH extraction and estimation of plasma flow in human postischemic acute renal failure. *Am J Physiol* 277: F312–F318, 1999
5. Ramaswamy D, Corrigan G, Polhemus C, Boothroyd D, Scandling J, Sommer FG, Alfrey E, Higgins J, Deen WM, Olshen R, Myers BD: Maintenance and recovery stages of postischemic acute renal failure in humans. *Am J Physiol Renal Physiol* 282: F271–F280, 2002
6. Olbricht C, Mason J, Takabatake T, Hohlbrugger G, Thurau K: The early phase of experimental acute renal failure. II. tubular leakage and the reliability of glomerular markers. *Pflugers Arch* 372: 251–258, 1977
7. Agarwal R: Chromatographic estimation of iothalamate and p-aminohippuric acid to measure glomerular filtration rate and effective renal plasma flow in humans. *J Chromatogr B Biomed Sci Appl* 705: 3–9, 1998
8. Florijn KW, Barendregt JN, Lentjes EG, van Dam W, Prodjosudjadi W, van Saase JL, van Es LA, Chang PC: Glomerular filtration rate measurement by "single-shot" injection of inulin. *Kidney Int* 46: 252–259, 1994
9. Agarwal R, Vasavada N, Chase SD: Liquid chromatography for iothalamate in biological samples. *J Chromatogr B Analyt Technol Biomed Life Sci* 785: 345–352, 2003
10. Erley CM, Bader BD, Berger ED, Vochazer A, Jorzik JJ, Dietz K, Risler T: Plasma clearance of iodine contrast media as a measure of glomerular filtration rate in critically ill patients. *Crit Care Med* 29: 1544–1550, 2001
11. Brandstrom E, Grzegorczyk A, Jacobsson L, Friberg P, Lindahl A, Aurell M: GFR measurement with iohexol and 51Cr-EDTA. A comparison of the two favoured GFR markers in Europe. *Nephrol Dial Transplant* 13: 1176–1182, 1998
12. Rabito CA, Moore RH, Bougas C, Dragotakes SC: Noninvasive, real-time monitoring of renal function: The ambulatory renal monitor. *J Nucl Med* 34: 199–207, 1993
13. Rabito CA, Panico F, Rubin R, Tolkoff-Rubin N, Teplick R: Noninvasive, real-time monitoring of renal function during critical care. *J Am Soc Nephrol* 4: 1421–1428, 1994
14. Muhler A: The future of contrast-enhanced magnetic resonance angiography. Are blood pool agents needed? *Invest Radiol* 33: 709–714, 1998
15. Chung JJ, Semelka RC, Martin DR: Acute renal failure: Common occurrence of preservation of corticomedullary differentiation on MR images. *Magn Reson Imaging* 19: 789–793, 2001
16. Mucelli RP, Bertolotto M, Quaia E: Imaging techniques in acute renal failure. *Contrib Nephrol* 132: 76–91, 2001
17. Szolar DH, Preidler K, Ebner F, Kammerhuber F, Horn S, Ratschek M, Ranner G, Petritsch P, Horina JH: Functional magnetic resonance imaging of human renal allografts during the post-transplant period: preliminary observations. *Magn Reson Imaging* 15: 727–735, 1997
18. Ruehm SG, Goyen M, Barkhausen J, Kroger K, Bosk S, Ladd ME, Debatin JF: Rapid magnetic resonance angiography for detection of atherosclerosis. *Lancet* 357: 1086–1091, 2001
19. Dupas B, Buzelin MF, Karam G, Vasse N, Meflah K, Bach-Gansmo T: Contrast-enhanced MR imaging of experimental acute tubular necrosis. *Acta Radiol* 42: 74–79, 2001
20. Brezis M, Rosen S: Hypoxia of the renal medulla—Its implications for disease. *N Engl J Med* 332: 647–655, 1995
21. Lieberthal W, Nigam SK: Acute renal failure. II. Experimental models of acute renal failure: Imperfect but indispensable. *Am J Physiol Renal Physiol* 278: F1–F12, 2000
22. Rosen S, Heyman SN: Difficulties in understanding human "acute tubular necrosis:" Limited data and flawed animal models. *Kidney Int* 60: 1220–1224, 2001
23. Prasad PV, Priatna A, Spokes K, Epstein FH: Changes in intrarenal oxygenation as evaluated by BOLD MRI in a rat kidney model for radiocontrast nephropathy. *J Magn Reson Imaging* 13: 744–747, 2001
24. Prasad PV, Edelman RR, Epstein FH: Noninvasive evaluation of intrarenal oxygenation with BOLD MRI. *Circulation* 94: 3271–3275, 1996
25. Laissy JP, Idee JM, Loshkajian A, Benderbous S, Chillon S, Beaufils H, Schouman-Claeys E: Reversibility of experimental acute renal failure in rats: assessment with USPIO-enhanced MR imaging. *J Magn Reson Imaging* 12: 278–288, 2000
26. Kobayashi H, Kawamoto S, Jo SK, Sato N, Saga T, Hiraga A, Konishi J, Hu S, Togashi K, Brechbiel MW, Star RA: Renal tubular damage detected by dynamic micro-MRI with a dendrimer-based magnetic resonance contrast agent. *Kidney Int* 61: 1980–1985, 2002
27. Kelly KJ, Molitoris BA: Acute renal failure in the new millennium: time to consider combination therapy. *Semin Nephrol* 20: 4–19, 2000
28. Star RA: Treatment of acute renal failure. *Kidney Int* 54: 1817–1831, 1998
29. Solez K, Racusen LC: Role of the renal biopsy in acute renal failure. *Contrib Nephrol* 68: 75, 2001
30. Jo SK, Hu X, Kobayashi H, Lizak M, Miyaji T, Koretsky A, Star RA: Detection of inflammation following renal ischemia by magnetic resonance imaging. *Kidney Int* 2003, in press
31. Kobayashi H, Sato N, Kawamoto S, Saga T, Hiraga A, Ishimori T, Konishi J, Togashi K, Brechbiel MW: Novel intravascular macromolecular MRI contrast agent with generation-4 polyamidoamine dendrimer core: Accelerated renal excretion with coinjection of lysine. *Magn Reson Med* 46: 457–464, 2001
32. Zhou H, Miyaji T, Kato A, Fujigaki Y, Sano K, Hishida A: Attenuation of cisplatin-induced acute renal failure is associated with less apoptotic cell death. *J Lab Clin Med* 134: 649–658, 1999
33. Kobayashi H, Kawamoto S, Jo SK, Brechbiel MW, Hu X, Yang T, Schnermann J, Star RA: Functional kidney imaging in mice: Using dendrimer based renal contrast agents [Abstract]. *J Am Soc Nephrol* 13: 143A, 2003
34. Kobayashi H, Kawamoto S, Jo SK, Bryant HL, Brechbiel MW, Star RA: Macromolecular MRI contrast agents with small dendrimers: Pharmacokinetic differences between sizes and cores. *Bioconjug Chem* 2003, in press
35. Miyaji T, Hu X, Star RA: alpha-Melanocyte-simulating hormone and interleukin-10 do not protect the kidney against mercuric chloride-induced injury. *Am J Physiol Renal Physiol* 282: F795–F801, 2002

36. Hauger O, Delalande C, Deminiere C, Fouqueray B, Ohayon C, Garcia S, Trillaud H, Combe C, Grenier N: Nephrotoxic nephritis and obstructive nephropathy: evaluation with MR imaging enhanced with ultrasmall superparamagnetic iron oxide-preliminary findings in a rat model. *Radiology* 217: 819–826, 2000
37. Ye Q, Yang D, Williams M, Williams DS, Pluempitiwiriyawej C, Moura JM, Ho C: In vivo detection of acute rat renal allograft rejection by MRI with USPIO particles. *Kidney Int* 61: 1124–1135, 2002
38. Zhang Y, Dodd SJ, Hendrich KS, Williams M, Ho C: Magnetic resonance imaging detection of rat renal transplant rejection by monitoring macrophage infiltration. *Kidney Int* 58: 1300–1310, 2000
39. Chiao H, Kohda Y, McLeroy P, Craig L, Housini I, Star RA: Alpha-melanocyte-stimulating hormone protects against renal injury after ischemia in mice and rats. *J Clin Invest* 99: 1165–1172, 1997
40. Denk W, Strickler JH, Webb WW: Two-photon laser scanning fluorescence microscopy. *Science* 248: 73–76, 1990
41. Denk W, Delaney KR, Gelperin A, Kleinfeld D, Strowbridge BW, Tank DW, Yuste R: Anatomical and functional imaging of neurons using 2-photon laser scanning microscopy. *J Neurosci Methods* 54: 151–162, 1994
42. Dunn KW, Sandoval RM, Kelly KJ, Dagher PC, Tanner GA, Atkinson SJ, Bacallao RL, Molitoris BA: Functional studies of the kidney of living animals using multicolor two-photon microscopy. *Am J Physiol Cell Physiol* 283: C905–C916, 2002
43. Brown EB, Campbell RB, Tsuzuki Y, Xu L, Carmeliet P, Fukumura D, Jain RK: In vivo measurement of gene expression, angiogenesis and physiological function in tumors using multiphoton laser scanning microscopy. *Nat Med* 7: 864–868, 2001
44. Kerr JF, Wyllie AH, Currie AR: Apoptosis: A basic biological phenomenon with wide-ranging implications in tissue kinetics. *Br J Cancer* 26: 239–257, 1972
45. Hengartner M: Apoptosis. Death by crowd control. *Science* 281: 1298–1299, 1998
46. Kelly KJ, Sandoval RM, Dunn KW, Molitoris BA, Dagher PC: A novel method to determine the specificity and sensitivity of the TUNEL reaction in the quantitation of apoptosis. *Am J Physiol Cell Physiol* 284: C1309–C1318. 2002
47. Dumont EA, Reutelingsperger CP, Smits JF, Daemen MJ, Doevendans PA, Wellens HJ, Hofstra L: Real-time imaging of apoptotic cell-membrane changes at the single-cell level in the beating murine heart. *Nat Med* 7: 1352–1355, 2001
48. Finucane DM, Bossy-Wetzel E, Waterhouse NJ, Cotter TG, Green DR: Bax-induced caspase activation and apoptosis via cytochrome c release from mitochondria is inhibitable by Bcl-xL. *J Biol Chem* 274: 2225–2233, 1999